I-EDU GROUP

Article

Unraveling the structural and electronic reorganization of oxidized cellulose: a density functional theory perspective on carboxyl-induced modifications

Makhliyo M.Kuzieva [1], Nurbek Sh.Ashurov *[1], Abdumutolib A.Atakhanov [1], Ilnar N. Nurgaliev [1], Anora Meylieva [2], Gofur B. Eshonqulov [2]

[1] Institute of Polymer Chemistry and Physics, Academy of sciences of the Republic of Uzbekistan, Tashkent, A. Kadiri street 7-b, Uzbekistan

[2] Faculty of Physics, National University of Uzbekistan named after Mirzo Ulugbek, Tashkent, 100174, Uzbekistan ansss72@mail.ru (N.A.), gb.eshonqulov@gmail.com (G.E.)

* Correspondence: ansss72@mail.ru Tel.: +998 93 5778072 (N.Sh. Ashurov)

Abstract: Controlled oxidation of cellulose introduces carboxyl functionalities at the C6 position, significantly modifying its hydrogen-bonding network, crystalline structure, and electronic properties. In this work, density functional theory (DFT) is employed to investigate pristine cellulose I and an oxidized model where the C6 hydroxymethyl group (–CHOH) is converted into a carboxyl group (–COOH), mimicking dichromate-induced oxidation. Structural optimization reveals anisotropic lattice distortion, including contraction along the a-axis, slight expansion along the b-axis, and increased lattice angles, indicating rearrangement of interchain packing. Hydrogen-bond analysis shows that oxidation increases the total number of hydrogen bonds from 18 to 24 while shortening the shortest H•••O distance from 1.78Å to 1.70Å, reflecting stronger intermolecular interactions. Bader charge analysis indicates significant electron depletion at the oxidized C6 sites, consistent with the electron-withdrawing nature of carboxyl groups. Electronic structure calculations reveal a reduction in the band gap and a downward shift of the chemical potential, suggesting enhanced electron-accepting behavior. Optical absorption spectra demonstrate increased intensity and pronounced anisotropy in the oxidized system. These findings provide atomistic insight into oxidation-induced transformations and establish a theoretical basis for designing functionalized cellulose materials with tailored properties.

Keyword: Oxidized nanocellulose, Carboxyl group, Structural transformation, Hydrogen bonding, Optical properties.

Quoting: Makhliyo M. Kuzieva, Nurbek Sh. Ashurov, Abdumutolib A. Atakhanov, Ilnar N. Nurgaliev, Anora Meylieva,r Gofur B. Eshonqulov. Unraveling the structural and electronic reorganization of oxidized cellulose: a density functional theory perspective on carboxyl-induced modifications. **2026**, 3, 1, 4. https://doi.org/

Received: 20.01.2026
Corrected: 30.01.2026
Accepted: 05.02.2026
Published: 13.02.2026

Introduction

Cellulose, the most abundant renewable polysaccharide, is a cornerstone for the development of sustainable functional materials due to its low cost, biodegradability, biocompatibility, and chemically versatile surface [1–3]. The transition from microstructured cellulose to nanocellulose has further amplified its technological relevance by drastically increasing specific surface area and exposing reactive sites, thereby enhancing interfacial phenomena such as adsorption and surface binding [4–6]. As a result, nanocellulose has emerged as a promising platform for environmentally benign sorbents and advanced composites [7–9]. However, pristine nanocellulose often lacks sufficient surface functionality and charge tunability, necessitating controlled chemical modification to optimize its interaction with target species [10–12].

Among modification strategies, controlled oxidation is particularly effective, as it enables the introduction of oxygen-containing functional groups while largely preserving the polysaccharide backbone [13–15]. Oxidation induces coupled transformations at both molecular and supramolecular levels: hydroxyl groups are converted into carbonyl and carboxyl functionalities, while the hydrogen-bonding network, crystallinity, and lattice organization are altered [16–18]. These multiscale structural changes govern key physicochemical properties, including swelling, porosity,

electrostatic interactions, and sorption performance [6,19,20]. Consequently, oxidized cellulose systems are actively explored for applications in adsorption, membrane technologies, catalysis, and biomedicine [8,9,21].

Oxidation using potassium dichromate in acidic media represents a chemically selective pathway, p erentially targeting less ordered regions of cellulose and promoting the conversion of primary hydroxyl groups at the C6 position into carboxyl functionalities [22]. This process is inherently heterogeneous, initiating at amorphous domains and crystalline surfaces before propagating into more ordered regions. Despite extensive experimental characterization by techniques such as X-ray diffraction and infrared spectroscopy, these methods cannot directly resolve the atomistic changes in bonding environment, charge redistribution, and electronic structure induced by oxidation.

In this context, density functional theory (DFT) provides a powerful framework for elucidating the fundamental mechanisms of cellulose modification. Atomistic modeling enables direct analysis of hydrogen-bond rearrangement, charge redistribution, and structural stability upon C6 oxidation, while electronic band structure and optical property calculations reveal changes inaccessible to conventional experiments.

In this work, we perform a DFT investigation of pristine cellulose Iβ and a model oxidized structure in which the C6 hydroxymethyl group is converted into a carboxyl group (–COOH), lecting dichromate-mediated oxidation pathways. The initial structure is based on the experimentally resolved cellulose Iβ crystal [23] and optimized under periodic boundary conditions using the GGA-PBE functional with Grimme's D3 dispersion correction and PAW pseudopotentials [24]. Calculations are carried out within the Atomistix Toolkit (ATK) framework [25,26]. By systematically comparing pristine and oxidized systems, we quantify changes in lattice parameters, hydrogen bonding characteristics, Bader charge distribution, electronic structure, and optical absorption.

This theoretical study provides atomistic insight into how C6-selective oxidation drives cooperative structural and electronic transformations in cellulose. The results bridge the gap between experimental observations and molecular-level understanding, offering a predictive basis for the rational design of oxidized cellulose materials with tailored functional properties.

Materials and Methods

Model Construction

The pristine cellulose model was constructed from the experimentally determined crystal structure of cellulose Iβ as reported by Nishiyama et al. [23], using the triclinic unit cell with atomic positions derived from high-resolution X-ray and neutron diffraction. The periodic model was built with the cell dimensions originally reported and subsequently optimized under periodic boundary conditions.

To simulate the oxidized system, the primary hydroxymethyl group (–CH_2OH) at the C6 position of selected glucose units was converted into a carboxyl group (–COOH). This modification reflects the experimentally observed preferential oxidation of C6 primary hydroxyl groups during potassium dichromate treatment. Both pristine and oxidized models were fully relaxed to enable a direct comparison of structural, electronic, and optical properties.

DFT Parameters

All calculations were performed using the ATK simulation package [25,26]. The exchange–correlation functional was treated within the generalized gradient approximation (GGA) using the Perdew–Burke–Ernzerhof (PBE) form [27]. Long-range van der Waals interactions were included via Grimme's D3 dispersion correction [24]. Electron–ion interactions were described by projector augmented wave (PAW) pseudopotentials with an accurate basis set for wavefunction expansion. The electrostatic potential and electron density were evaluated on a real-space grid with a mesh cutoff energy of 6000 eV.

Brillouin zone integration was performed using a k-point density of 7 $Å^{-1}$, corresponding to a $5 \times 6 \times 5$ Monkhorst–Pack grid for the optimized unit cell. Electronic occupations were smeared using the Fermi–Dirac distribution with a broadening of 100 K. Spin-unpolarized configurations and neutral charge states were assumed. Structural relaxations continued until the maximum residual force on any atom fell below 0.01 eV $Å^{-1}$.

Optical Calculations

Optical properties were computed using the frequency-dependent susceptibility tensor within the Kubo–Greenwood formalism:

$$\chi_{i,j}(\omega) = -\frac{e^2\hbar^4}{m^2\varepsilon_0 V\omega^2}\sum_{n,m}\frac{f(E_m)-f(E_n)}{E_{nm}-\hbar\omega-i\hbar\Gamma}\pi^i_{nm}\pi^j_{mn} \quad (2)$$

where f is the Fermi–Dirac distribution, π^i_{nm} is the i-component of the dipole matrix element, Γ is the energy broadening parameter, and V is the unit-cell volume. The complex dielectric function is defined as

$$\varepsilon(\omega) = \varepsilon_1(\omega) + i\varepsilon_2(\omega) = 1 + \chi(\omega).$$

The complex refractive index $n + ik$ is obtained from the dielectric function as

$$n + ik = \sqrt{\varepsilon} \quad (3)$$

The optical absorption coefficient α_0 is calculated using

$$\alpha_0 = \frac{2\omega}{c}k \quad (4)$$

All calculations were performed using the Atomistix Toolkit simulation package [25,26].

Results

To complement the experimental observations and provide molecular-level insight into the structural effects of oxidation, density functional theory simulations were performed for pristine and oxidized cellulose models. While X-ray diffraction and FTIR spectroscopy reveal macroscopic changes in crystallinity and hydrogen-bond interactions, these techniques cannot directly resolve how chemical modification alters the local bonding environment and electronic structure of the cellulose lattice. Atomistic simulations therefore enable direct examination of how oxidation at the C6 position affects the hydrogen-bond network, charge distribution, and structural stability of cellulose chains. By comparing pristine and oxidized models, the calculations provide a microscopic interpretation of the experimentally observed changes in hydrogen bonding, lattice parameters, and functional group formation.

Figure 1 presents the atomic models used in the simulations to investigate the structural effects of oxidation on cellulose. The pristine cellulose model (Fig. 1a) represents the crystalline cellulose structure containing the native hydroxymethyl group (–CH_2OH) attached to the C6 position of the glucose units. The cellulose chains form the characteristic layered arrangement stabilized by a dense network of intra- and intermolecular hydrogen bonds.

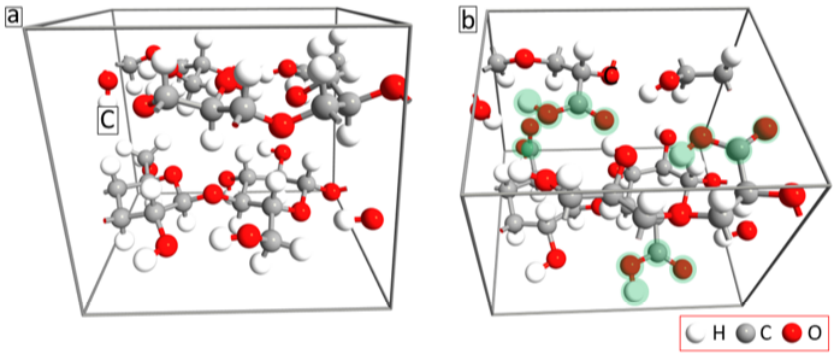

Figure 1. Atomic structures of the cellulose model before and after oxidation. (a) Pristine cellulose structure containing the native C6 hydroxymethyl group (–CH_2OH) attached to the glucose units. (b) Oxidized cellulose structure obtained by converting the C6 hydroxymethyl group into a carboxyl group (–COOH). The atoms belonging to the newly introduced –COOH functional groups are highlighted to indicate the oxidation sites.

To simulate the oxidation process observed experimentally, the C6 hydroxymethyl group was converted into a carboxyl group (–COOH), resulting in the oxidized cellulose model shown in Fig. 1b. The atoms belonging to the newly introduced carboxyl groups are highlighted to indicate the oxidation sites. This modification reflects the preferential oxidation of primary hydroxyl groups at the C6 position during dichromate treatment. The constructed models therefore enable direct comparison of the pristine and oxidized structures and allow analysis of how the introduction of carboxyl groups alters the hydrogen-bond network and local electronic environment of the cellulose lattice.

The effect of oxidation on the crystalline structure of cellulose was further analyzed by comparing the optimized lattice parameters of the pristine and oxidized models. The relaxed pristine cellulose structure exhibits triclinic symmetry with lattice parameters $a = 9.35\,\text{Å}$, $b = 8.31\,\text{Å}$, and $c = 10.46\,\text{Å}$, and lattice angles $\alpha = 87.16^\circ$, $\beta = 86.56^\circ$, and $\gamma = 93.72^\circ$. These values are consistent with the experimentally reported crystal structure of cellulose Iβ and confirm that the computational model reliably reproduces the structural characteristics of native cellulose.

After introducing oxidation at the C6 position, noticeable changes in the lattice parameters are observed. The oxidized cellulose structure remains triclinic but shows modified cell dimensions of $a = 7.71\,\text{Å}$, $b = 8.52\,\text{Å}$, and $c = 10.38\,\text{Å}$, with lattice angles $\alpha = 92.79^\circ$, $\beta = 95.17^\circ$, and $\gamma = 97.15^\circ$. Compared with the pristine system, the a lattice parameter decreases, while the b parameter slightly increases, and the c parameter remains nearly unchanged. At the same time, the lattice angles increase, indicating a distortion of the unit cell geometry.

These structural changes can be attributed to the conversion of the C6 hydroxymethyl group (–CH_2OH) into a carboxyl group (–COOH). The introduction of the more polar and sterically different carboxyl functionality modifies the local hydrogen-bond network and alters intermolecular interactions between neighboring cellulose chains. As a result, the packing of the chains within the crystal lattice becomes slightly rearranged, leading to the observed anisotropic variation of the lattice parameters. Such structural adjustments are consistent with experimental XRD results, which indicate modifications in crystallinity and lattice organization during the oxidation process.

Table 1. Comparison of hydrogen-bond characteristics in pristine and oxidized cellulose obtained from DFT calculations, including the total number of hydrogen bonds, the shortest H···O interaction distance, and the corresponding structural effect on the hydrogen-bond network.

System	Number of H-bonds	Shortest H···O (Å)	Structural effect
Pristine cellulose	18	1.78	intrachain H-bond network
Oxidized cellulose	24	1.70	stronger interchain bonding

Hydrogen bonding plays a fundamental role in determining the structural stability and packing of cellulose chains within the crystalline lattice. The extensive network of intra- and intermolecular hydrogen bonds stabilizes the supramolecular architecture of cellulose and strongly influences its mechanical and physicochemical properties. Table 1 summarizes the hydrogen-bond characteristics obtained from the DFT calculations for the pristine and oxidized cellulose models. The pristine cellulose structure contains 18 hydrogen bonds, with the shortest H$\cdots$O distance of 1.78 Å, reflecting the typical intrachain hydrogen-bond network that stabilizes native cellulose. After oxidation, the total number of hydrogen bonds increases to 24, while the shortest H$\cdots$O distance decreases to 1.70 Å, indicating stronger hydrogen-bond interactions. This increase in hydrogen bonding arises from the introduction of carboxyl (–COOH) groups at the C6 position, which provide additional hydrogen-bond donors and acceptors. As a result, oxidation promotes stronger interchain interactions, leading to a redistribution of the hydrogen-bond network within the cellulose lattice. This structural rearrangement is consistent with the experimentally observed modifications in the hydrogen-bond environment derived from FTIR analysis.

Table 2. Comparison of hydrogen-bond characteristics in pristine and oxidized cellulose obtained from DFT calculations, including the total number of hydrogen bonds, the shortest H···O interaction distance, and the corresponding structural effect on the hydrogen-bond network.

Atom type	Pristine (e)	Oxidized (e)	Change (Oxidized Pristine) (e)
C6	0.454	1.510	**1.056**
C5	0.414	0.398	**+0.016**
O	+1.057	+1.054	**0.003**
H	0.562	0.560	**+0.002**

Charge analysis provides important insight into how oxidation modifies the local electronic structure of cellulose and helps identify regions where electron redistribution occurs after chemical functionalization. Table 2 presents the Bader charge values for representative atoms in the pristine and oxidized cellulose models. The most significant charge change occurs at the C6 atoms, where the charge decreases by approximately -1.06 e after oxidation. This pronounced variation indicates strong electron depletion at the C6 site, which is consistent with the electron-withdrawing character of the introduced carboxyl (–COOH) groups formed during oxidation. In contrast, the neighboring C5 atoms, as well as the oxygen and hydrogen atoms associated with the hydroxyl groups, show only minor charge variations. This behavior suggests that the electronic redistribution induced by oxidation is largely localized around the modified C6 positions, while the electronic environment of the surrounding cellulose framework remains relatively unchanged. Such localized charge redistribution supports the proposed oxidation mechanism and helps explain the changes in intermolecular interactions and hydrogen bonding observed in the oxidized cellulose structure.

To investigate the effect of oxidation on the electronic properties of cellulose, the electronic band structures of the pristine and oxidized models were calculated using DFT. Figure 2 shows the band dispersions of (a) pristine cellulose and (b) oxidized cellulose along the high-symmetry path Y—X–V–U–R–Z–T in the Brillouin zone. In both systems, the bands exhibit relatively weak dispersion, which is characteristic of molecular crystals where electronic states are largely localized within the polymer chains.

For the pristine cellulose structure, the calculated Fermi level is located at -3.41 eV, and the system exhibits a wide indirect band gap of 4.70 eV (direct gap 4.71 eV), confirming the insulating nature of native cellulose. The valence band maximum (VBM) and conduction band minimum (CBM) are located at -2.35 eV and 2.34 eV, respectively. These results indicate that pristine cellulose possesses a large electronic band gap typical of organic polymeric materials dominated by localized σ-bonding states.

After oxidation, noticeable changes in the electronic structure are observed. In the oxidized cellulose model, the Fermi level shifts to -4.28 eV, and the band gap decreases to 3.73 eV (direct gap 3.79 eV). The valence and conduction band edges are located at -1.87 eV and 1.87 eV, respectively. The reduction of the band gap suggests that the introduction of carboxyl (–COOH) groups modifies the electronic states near the band edges, likely due to the strong electron-withdrawing character and increased polarity of the oxygen-containing functional groups. These modifications introduce additional electronic interactions within the cellulose lattice, leading to a narrowing of the band gap.Overall, the results indicate that oxidation significantly influences the electronic structure of cellulose by reducing the band gap and shifting the Fermi level, while the overall insulating character of the material is preserved. Such changes in the electronic structure may influence charge distribution and intermolecular interactions in oxidized cellulose, which can affect its chemical reactivity and interaction with surrounding molecules.

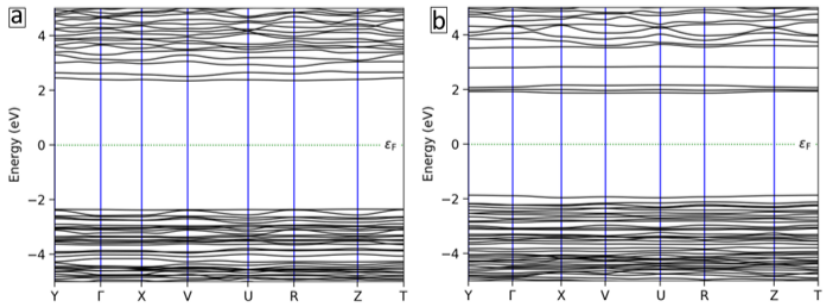

Figure 2. Electronic band structures of (a) pristine cellulose and (b) oxidized cellulose obtained after converting the C6 hydroxymethyl group (–CHOH) into a carboxyl group (–COOH). The band dispersions are plotted along the high-symmetry path Y—X–V–U–R–Z–T in the Brillouin zone. The dashed green horizontal line indicates the Fermi level, which is set to 0 eV.

Evaluation of the chemical potential provides additional insight into the electronic stability and charge-transfer characteristics of a material. In DFT calculations, the chemical potential is closely related to the Fermi level and represents the energy required to add or remove electrons from the system. Therefore, it serves as an important indicator of the tendency of a structure to donate or accept electronic charge.

For the pristine cellulose model, the calculated chemical potential is 3.41 eV, whereas for the oxidized cellulose structure it decreases to 4.28 eV. The shift toward more negative values after oxidation indicates a lowering of the electronic energy level of the system. This behavior is consistent with the introduction of electron-withdrawing carboxyl (–COOH) groups, which stabilize the electronic states and increase the electron-accepting character of the oxidized cellulose. Consequently, the oxidized structure exhibits a stronger tendency to attract electrons compared with the pristine cellulose model. This result is in agreement with the Bader charge analysis and band structure calculations, which also indicate significant electronic redistribution around the oxidized C6 sites.

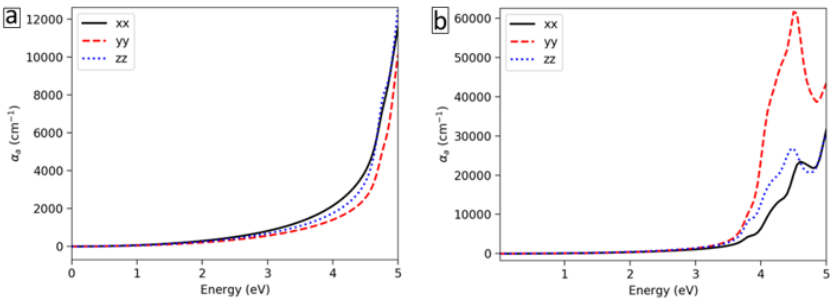

Figure 3. Calculated optical absorption spectra of (a) pristine cellulose and (b) oxidized cellulose obtained by converting the C6 hydroxymethyl group (–CH_2OH) into a carboxyl group (–COOH). The spectra are derived from the frequency-dependent dielectric function and represent the photon-energy-dependent absorption coefficient.

To further investigate the influence of oxidation on the optical properties of cellulose, the optical absorption spectra of the pristine and oxidized models were calculated from the frequency-dependent dielectric function. Figure 5 presents the photon-energy-dependent absorption coefficient along the three principal crystallographic directions (xx, xy, and zz) for (a) pristine cellulose and (b) oxidized cellulose.

For the pristine cellulose structure (Fig. 3a), the absorption coefficient remains very small at low photon energies and increases gradually with increasing energy. A significant rise in absorption occurs at photon energies above approximately 4 eV, which corresponds well with the large electronic band gap obtained from the band structure calculations. The absorption profiles along the xx, xy, and zz directions are relatively similar, indicating weak anisotropy in the optical response of the pristine cellulose lattice.

In contrast, the oxidized cellulose structure (Fig. 3b) exhibits a markedly enhanced optical absorption intensity, particularly in the higher energy region. Strong absorption peaks appear in the

range of approximately 4–4.5 eV, with the xy polarization showing the largest absorption coefficient, exceeding 6×10^4 cm^{-1}. The xx and zz components also display increased absorption compared with the pristine system, although their intensities are lower than that of the xy direction. This pronounced increase in absorption is consistent with the reduction of the band gap observed in the oxidized cellulose model, which allows optical transitions to occur at lower photon energies.

Overall, the results indicate that oxidation significantly modifies the optical response of cellulose by increasing the absorption intensity and introducing stronger anisotropy in the optical spectra. These changes originate from the presence of carboxyl (–COOH) groups, which alter the electronic structure and introduce additional electronic states near the band edges, thereby facilitating optical transitions.

Conclusions

Density functional theory simulations provide atomistic insight into these structural changes. The calculations show that conversion of the C6 hydroxymethyl group into a carboxyl group modifies the hydrogen-bond network, increasing the number and strength of intermolecular interactions. Structural relaxation reveals noticeable changes in lattice parameters, while Bader charge analysis indicates strong electron depletion at the oxidized C6 sites. In addition, oxidation reduces the electronic band gap and shifts the chemical potential to lower energies, accompanied by enhanced optical absorption in the oxidized structure.

Overall, the combined experimental and theoretical results demonstrate that oxidation induces cooperative structural and electronic rearrangements within the cellulose lattice. These findings provide fundamental insight into how controlled oxidative functionalization modifies the crystalline structure and hydrogen-bonding architecture of cellulose, offering guidance for tailoring oxidized celluloses for advanced applications.

Authors' contribution

Makhliyo M. Kuzieva: Investigation, validation, writing – original draft. Nurbek Sh. Ashurov: Conceptualization, investigation, methodology, visualization, writing – original draft, writing – review editing. Abdumutolib A. Atakhanov: Conceptualization, supervision, data curation, formal analysis, validation, writing – review editing. Ilnar N. Nurgaliev - Investigation, formal analysis writing – original draft. Gofur B. Eshonqulov: - Formal analysis, writing – review editing

Funding source

This research was supported by the Basic Fundamental Program of the Academy of Sciences of the Republic of Uzbekistan, the Uzbekistan–Belarus joint project funded by the Ministry of Higher Ed-ucation, Science and Innovation of the Republic of Uzbekistan (Grant No. FL-8824063308).

Ethics approval.

Since this study does not involve human or animal subjects, ethical review and approval is notrequired. Therefore, ethical approval does not apply to research.

Consent for publication

Human participants were not involved in this study. For this reason, informed consent is not required.

Data Availability Statement

All experimental data confirming the results presented in this article are held by the authors and presented within the article in the form of the main text and image/table. Additional information can be obtained from the author(s)based on a reasoned query

Acknowledgments

The authors thank the team of the Institute of Polymer Chemistry and Physics, which provided technical assistance in the implementation of this research.

Conflict of interest

The authors declare that there is no conflict of interest in this study. There are no personal, financial or other interests that affect the presentation or interpretation of research results.

Abbreviations

DFT	density functional theory
ATK	Atomistix Toolkit
GGA	Generalized Gradient Approximation
PBE	Perdew–Burke–Ernzerhof functional
PAW	projector augmented wave
VBM	Valence Band Maximum
CBM	Conduction Band Minimum
f	Fermi–Dirac distribution
α_0	optical absorption coefficient

References

[1] C. Huang, H. Yu, Y. Gao, Y. Chen, S. Y. H. Abdalkarim, K. C. Tam. Recent advances in green and efficient cellulose utilization through structure deconstruction and regeneration. Adv. Funct. Mater. 35, 2424591 (2025).

[2] F. Shahi, H. Moshiri, F. Kamran, H. Afshar. Superabsorbent polymers: emerging functionalities and their role in advancing technologies. Polym. Eng. Sci. (2025).

[3] C. M. Altaner, L. H. Thomas, A. N. Fernandes, M. C. Jarvis. How cellulose stretches: synergism between covalent and hydrogen bonding. Biomacromolecules 15, 791–798 (2014).

[4] A. Dufresne. Nanocellulose: a new ageless bionanomaterial. Mater. Today 16, 220–227 (2013).

[5] N. Mahfoudhi, S. Boufi. Nanocellulose as a novel nanostructured adsorbent for environmental remediation: a review. Cellulose 24, 1171–1197 (2017).

[6] G. X. Lan, Y. Liu, N. Zhou, D. Q. Guo, M. G. Ma. Multifunctional nanocellulose-based composites for potential environmental applications. Cellulose 30, 39–60 (2023).

[7] M. N. F. Norrrahim, N. A. M. Kasim, V. F. Knight, M. S. M. Misenan, N. Janudin, N. A. A. Shah, W. M. Z. W. Yunus. Nanocellulose: a bioadsorbent for chemical contaminant remediation. RSC Adv. 11, 7347–7368 (2021).

[8] M. M. Alighanbari, F. Danafar, A. Namjoo, A. Saeed. Recent advances in the applications of nanocellulose for sustainable development. Express Polym. Lett. 19, 15–46 (2025).

[9] M. Fernandes, C. Alves, L. Melro, R. D. Fernandes, J. Padrão, A. J. Salgado, A. Zille. Modification of nanocellulose. In: Handbook of Biomass, 1–39 (2023).

[10] N. M. Nurazzi, R. A. Ilyas, S. M. Sapuan (Eds.). Synthetic and Natural Nanofillers in Polymer Composites: Properties and Applications. Elsevier (2023).

[11] R. Wang, Y. Feng, D. Li, K. Li, Y. Yan. Towards the sustainable production of biomass-derived materials with smart functionality: a tutorial review. Green Chem. 26, 9075–9103 (2024).

[12] C. Huang, Q. Qin, Y. Liu, G. Duan, P. Xiao, Y. Huang, S. Jiang. Physicochemical, polymeric and microbial modifications of wood toward advanced functional applications: a review. Chem. Soc. Rev. 54, 9027–9091 (2025)

[13] S. Liyanage, S. Acharya, P. Parajuli, J. L. Shamshina, N. Abidi. Production and surface modification of cellulose bioproducts. Polymers 13, 3433 (2021).

[14] A. Potthast, T. Rosenau, P. Kosma. Analysis of oxidized functionalities in cellulose. Polysaccharides II, 1–48 (2006).

[15] K. Ariga, S. Ishihara, J. Labuta, J. P. Hill. Supramolecular approaches to nanotechnology: switching properties and dynamic functions. Curr. Org. Chem. 15, 3719–3733 (2011).

[16] D. V. Bhalani, B. Nutan, A. Kumar, A. K. Singh Chandel. Bioavailability enhancement techniques for poorly aqueous soluble drugs and therapeutics. Biomedicines 10, 2055 (2022).

[17] B. Qian, Z. Chang, X. H. Bu. Functionalized dynamic metal-organic frameworks as smart switch for sensing and adsorption applications. In: Metal-Organic Framework: From Design to Applications, 135–173 (2019).

[18] F. Azzam, C. Moreau, F. Cousin, A. Menelle, H. Bizot, B. Cathala. Cellulose nanofibril-based multilayered thin films: effect of ionic strength on porosity, swelling, and optical properties. Langmuir 30, 8091–8100 (2014).

[19] M. Pagliaro, R. Ciriminna, M. Yusuf, S. Eskandarinezhad, I. A. Wani, M. Ghahremani, Z. R. Nezhad. Application of nanocellulose composites in environmental engineering as catalysts, flocculants, and energy storage materials: a review. J. Compos. Compd. 3, 114–128 (2021).

[20] M. Kuzieva, A. Atakhanov, S. Shaxabutdinov, N. Ashurov, K. Yunusov, G. Jiang. Preparation of oxidized nanocellulose using potassium dichromate. Cellulose 30, 5657–5668 (2023).

[21] M. M. Kuzieva, F. M. Urishova, A. A. Atakhanov, N. S. Ashurov, S. S. Rashidova, D. I. Shiman, S. Kang. Potassium permanganate–oxidized nanocellulose: structural features and rheological performance for advanced applications. Eurasian J. Chem. 30, 148–159 (2025).
[22] J. Kang, X. Yang, Q. Hu, Z. Cai, L. M. Liu, L. Guo. Recent progress of amorphous nanomaterials. Chem. Rev. 123, 8859–8941 (2023).
[23] Y. Nishiyama, P. Langan, H. Chanzy. Crystal structure and hydrogen-bonding system in cellulose I from synchrotron X-ray and neutron fiber diffraction. J. Am. Chem. Soc. 124, 9074–9082 (2002).
[24] S. Grimme, Semiempirical GGA-type density functional constructed with a long-range dispersion correction, J. Comput. Chem. 27 (2006) 1787.
[25] S. Smidstrup, T. Markussen, P. Vancraeyveld, J. Wellendorff, J. Schneider, T. Gunst, B. Verstichel, D. Stradi, P.A. Khomyakov, U.G. Vej-Hansen, QuantumATK: An integrated platform of electronic and atomic-scale modelling tools, J. Phys.: Condens. Matter 32 (2020) 015901.
[26] S. Smidstrup, D. Stradi, J. Wellendorff, P.A. Khomyakov, U.G. Vej-Hansen, M.-E. Lee, T. Ghosh, E. Jónsson, H. Jónsson, K. Stokbro, First-principles Green's-function method for surface calculations: A pseudopotential localized basis set approach, Phys. Rev. B 96 (2017) 195309.
[27] J.P. Perdew, K. Burke, M. Ernzerhof, Generalized Gradient Approximation Made Simple, Phys. Rev. Lett. 77 (1996) 3865